Comparative Medicine
Copyright 2011
by the American Association for Laboratory Animal Science

Vol 61, No 5
October 2011
Pages 441–444

Case Report

Renal Failure Associated with Mucopolysaccharidosis Type I in a Cat from a MPS I Research Colony

Rachel E Cianciolo,[1,*] James L Rhodes,[2] Mark E Haskins,[3] Fred J Clubb,[4] and George E Lees[5]

Renal failure was diagnosed in an 11-mo-old male domestic shorthair cat from a colony with mucopolysaccharidosis type I lysosomal storage disease. Grossly, the kidneys were enlarged and bulged on cut section. Histology revealed tubular necrosis and regeneration with severe interstitial macrophage accumulation. Tubular epithelial cells and interstitial macrophages were distended by abundant, large cytoplasmic vacuoles. Electron microscopy demonstrated severe tubular epithelial vacuolar degeneration with lysosomes distended by granular debris and mineral precipitates. Interstitial macrophages contained similarly distended lysosomes. Although the initial cause of the tubular injury was not identified, the presence of macrophages laden with storage product most likely exacerbated the disease. The macrophage infiltrate may have caused tubular ischemia by compressing peritubular capillaries and separating tubules from their blood supply. Because the kidney is not normally affected in MPS I, this case is an unusual presentation of a well-characterized disease. Furthermore, this report documents the diagnostic workflow used to investigate a single case of feline acute renal failure in the setting of numerous at-risk laboratory animals.

Abbreviations: GAG, glycosaminoglycan; MPS I, mucopolysaccharidosis type I.

Mucopolysaccharidosis type I (MPS I) is a lysosomal storage disease caused by deficient activity of α-$_L$-iduronidase, an enzyme required for the degradation of the glycosaminoglycans (GAG) heparan and dermatan sulfates.[1] Lack of functional α-$_L$-iduronidase results in accumulation of GAG in the nervous, musculoskeletal, hepatobiliary, and cardiovascular systems.[4] In humans, the disease is manifested as Hurler, Hurler–Scheie, and Scheie syndromes, which have severe, intermediate, or attenuated lesions, respectively.[1] Three animal models (canine,[10] feline,[4] and murine[3]) exist, and colonies of affected cats have been established and maintained at the University of Pennsylvania for the purpose of understanding its pathogenesis and developing safe, effective treatment of this ultimately fatal disease.[4]

Clinical evaluation of MPS I cats reveals facial dysmorphia, corneal clouding, gait abnormalities, multiple skeletal defects, and occasional heart murmurs. Clinicopathologic findings include excess urinary dermatan sulfate and heparan sulfate.[4] Lysosomal storage of GAG has been documented in renal tubular epithelial cells of mice[3] and cats[4] with MPS I; however, neurons, hepatocytes, chondrocytes, smooth muscle cells, WBC, and fibroblasts of the heart valves, skin, and eye are the predominant cell types affected.[4] To our knowledge, renal failure has not been reported in MPS I cats. We describe the clinical, histopathologic, and ultrastructural evaluation of an 11-mo-old intact male cat with MPS I that developed renal failure associated with significant lysosomal storage material within renal tubular epithelial cells and interstitial macrophages.

Received: 09 Nov 2010. Revision requested: 27 Jan 2011. Accepted: 16 Feb 2011.
[1]Department of Public Health and Pathobiology, North Caroline State University, Raleigh, North Carolina; [2]Departments of University Laboratory Animal Research and [3]Pathobiology and Clinical Studies, University of Pennsylvania, Philadelphia, Pennsylvania; [4]Departments of Pathobiology and [5]Small Animal Clinical Studies, Texas A&M University, College Station, Texas.
[*]Corresponding author: Email: recianci@ncsu.edu

Case Report

An 11-mo-old intact male MPS-I-affected cat from the MPS I colony at the University of Pennsylvania, School of Veterinary Medicine, was examined for weight loss and inappetance. The feline colony was maintained in accordance with study protocols reviewed and approved by the University of Pennsylvania Laboratory Animal Care Committee. The cat had lost 0.7 kg over the period of 1 mo. Clinical examination revealed moderate dehydration and ulcerated buccal mucosa at the right oral commissure. Over the course of 5 d, the cat received subcutaneous fluids and antibiotics (62.5 mg/kg PO twice daily; Clavamox, Pfizer, New York, NY). During this time, he was syringe-fed canned food (Science Diet A/D, Hills Pet Nutrition, Topeka, KS) mixed with water, and he occasionally ate on his own. After 3 d with no improvement in appetite or hydration status, an additional antibiotic (5 mg/kg IM once daily; Baytril, Bayer, Pittsburgh, PA) was administered for 3 d. At this time, the cat began to drag his right hindlimb and seemed painful; an analgesic (0.01 mg/kg SC; Buprenex, Reckitt Benckiser Pharmaceuticals, Richmond, VA) was given. Blood was drawn for a CBC and serum chemistry screen, and urine was collected via cystocentesis. No abnormalities were seen in the CBC. Serum chemistry revealed severely elevated blood

urea nitrogen (268 mg/dL), creatinine (5.7 mg/dL), phosphate (24.3 mg/dL), sodium (167 mEq/L), and globulins (5.1 g/dL). Urinalysis demonstrated inadequate urine concentrating ability with a urine specific gravity of 1.008. Small irregularly shaped crystals were present in the urine.

Due to the progression of clinical signs despite treatment, the cat was euthanized with an overdose of barbiturate, and a necropsy was performed. The kidneys were removed first, and samples (1 to 2 mm^3) for electron microscopy were placed in chilled 3% gluteraldehyde within 5 min of euthanasia. Additional sections of kidney were placed in buffered 10% formalin for light microscopic evaluation. Grossly, the kidneys were slightly enlarged and bulged when sectioned. The liver was diffusely pale tan and enlarged, weighing 4.6% body weight. All other organs were grossly normal; representative tissue samples were harvested and placed in formalin. Formalin-fixed kidney was processed routinely, embedded in paraffin, sectioned at 3 µm, and stained with hematoxylin and eosin, periodic acid Schiff, and Masson trichrome. Immunohistochemistry was performed on formalin-fixed paraffin-embedded sections as described previously,[5,6] using a monoclonal antiCD18 antibody (ThermoScientific, Rockford, IL) and a polyclonal rabbit antibody against osteopontin (Abcam, Cambridge, MD). Additional sections of formalin-fixed kidney that had not been processed for paraffin embedding were stained with oil red O for detection of lipid. Samples for electron microscopy were sent to the Texas Veterinary Renal Pathology Service and processed routinely.

Histopathology of the kidney (Figures 1 and 2) revealed severe expansion of the interstitium by large numbers of macrophages, which contained cytoplasmic vacuoles that displaced the nucleus to the periphery of the cell. Admixed with these macrophages were scattered lymphocytes and plasma cells. Tubules were frequently dilated and lined by attenuated to cuboidal epithelial cells. Proximal tubular epithelium often lacked an apical brush border, and most tubular epithelial cells contained small (2 to 3 µm) or large (6 to 8 µm) cytoplasmic vacuoles. Because this vacuolation was diffuse throughout the nephron and because the presence of the vacuoles often distorted the cell shape, the lesion was not consistent with feline proximal tubular lipidosis that occurs in normal cats. Basophilic crystalline material occasionally was present within the dilated tubules or within the interstitium adjacent to ruptured tubules (Figure 2). Many tubules were lined by basophilic and karyomegalic epithelial cells, suggestive of regeneration, whereas scattered, fewer tubular cross-sections were overtly necrotic. Glomerular tufts were normal. Immunohistochemistry for CD18 (Figure 3) verified that the interstitial cells were leukocytes and not distended fibroblasts. Oil red O stains of tissue revealed abundant lipid within most of the aforementioned vacuoles, consistent with previous reports.[4]

Light microscopic evaluation of additional tissues revealed similar vacuoles within the cytoplasm of cerebellar neuronal cell bodies, hepatocytes, Kupffer cells, and bronchial chondrocytes. In addition, there were occasional foci of vacuolated macrophages in lymph nodes, around cerebral and cerebellar vessels, and in the lamina propria of the intestine. All other organs were histologically normal.

Electron microscopic evaluation of the renal cortex (Figure 4) revealed severe tubular epithelial vacuolar degeneration. Specifically, there was blunting and loss of microvilli of the proximal tubules as well as occasional blebbing of the apical membrane of all segments of the nephron. Epithelial cells of the distal tubules were characterized by the presence of large numbers of membrane bound inclusions containing granular material, with or without the presence of irregularly shaped electron dense precipitates. This material was ultrastructurally consistent with mineral, most likely calcium precipitates. The proximal tubules were mildly, but similarly, affected. Singly necrotic or apoptotic cells were frequent, especially within the distal nephron. The interstitium was multifocally expanded by collagen and numerous macrophages distended by similar lysosomes containing lipid and granular debris (Figure 4).

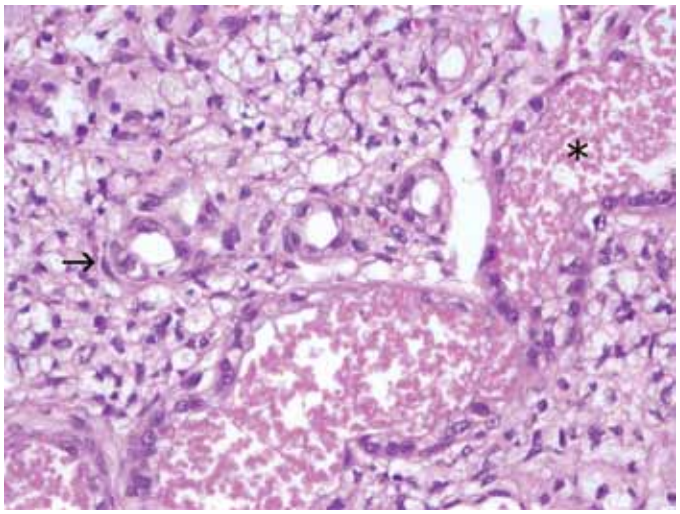

Figure 1. Photomicrograph of cortical renal tubules from a cat with MPS-I-associated renal failure. Nonatrophic tubules are moderately dilated, and sloughed cellular debris is within tubular lumens (*). A tubule with necrotic epithelial cells (arrow) is undergoing atrophy. The interstitium is severely expanded by vacuolated macrophages. Hematoxylin and eosin stain; magnification, ×40.

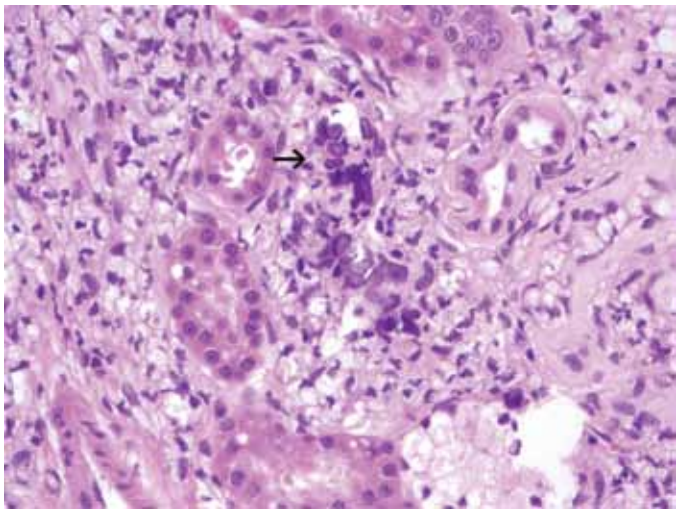

Figure 2. Photomicrograph of basophilic mineralized crystals within a ruptured tubule (arrow). Hematoxylin and eosin stain; magnification, ×40.

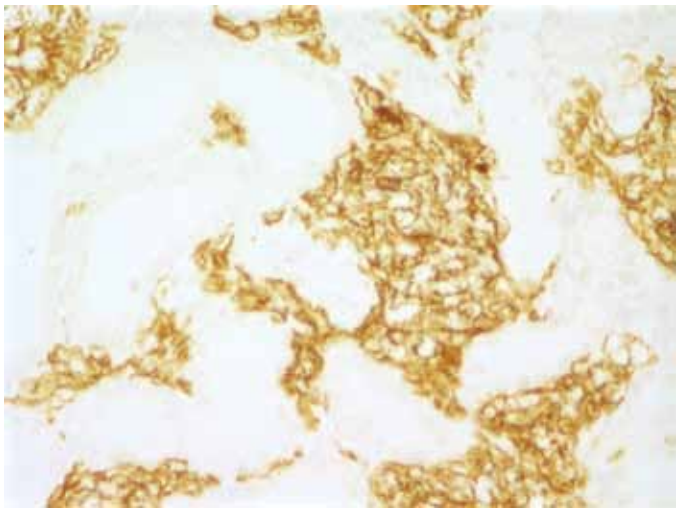

Figure 3. Photomicrograph of the kidney stained immunohistochemically with antiCD18 antibody, revealing that the interstitial cells are leukocytes, consistent with macrophages. Magnification, ×40.

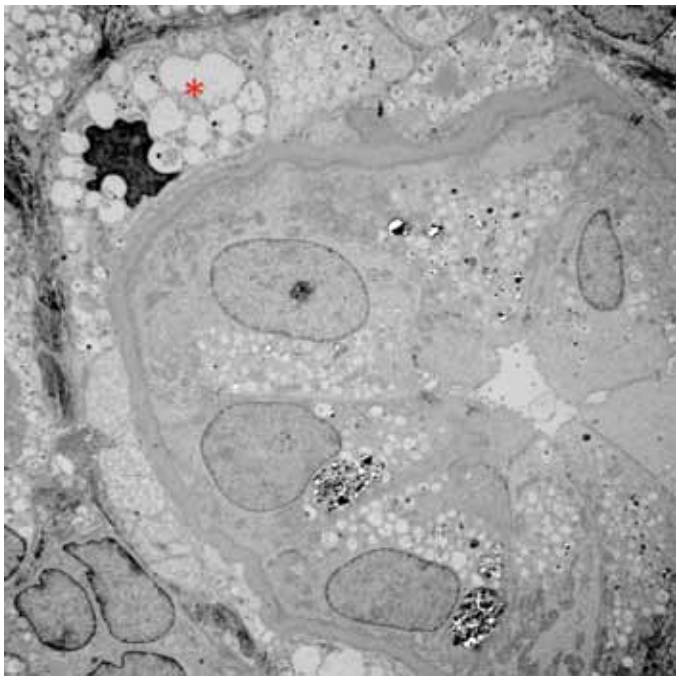

Figure 4. Electron micrograph of a collecting duct from a cat with MPS-I-associated renal failure. Tubular epithelial cells contain lysosomes distended by granular material, lipid, and electron dense precipitates. The interstitial macrophage (*) contains similar material.

Discussion

The presence of numerous vacuolated tissue macrophages in histologic sections is suggestive of a lysosomal storage disease. In MPS I, phagolysosomes are distended not only by the presence of GAG but also by lipid, as demonstrated by positive Oil red O staining.[4] Although 'zebra bodies' were not identified ultrastructurally in the current case, their presence is not required for diagnosis of lysosomal storage disease. In a previous report,[4] zebra bodies were limited to the liver and CNS, whereas monocytes and fibroblasts contained lysosomes distended by granular material, similar to those in the present case.

The cause of the tubular necrosis in our cat is currently unknown. Tubular necrosis is often secondary to toxin exposure or ischemia. Because the cat was a laboratory animal, exposure to toxins (ethylene glycol, lilies, or aminoglycoside antibiotics) was not likely. Furthermore, no other cats were affected. Food samples and urine were examined for the presence of melamine and cyanuric acid and were negative. In addition, there were no gold-brown circular crystals characteristic of melamine–cyanuric acid exposure in histologic samples. The absence of clinically evident cardiac disease and histologic lesions in the heart suggest that the tubular necrosis was not secondary to ischemia from heart failure. In addition, tubular necrosis was not due to anemia, because the RBC count was within normal limits.

The presence of crystals in urine and kidney suggest that crystalluria may have been involved in the pathogenesis of the tubular necrosis. Urolithiasis in pet cats has increased in prevalence and is considered to be the result of multiple interacting elements (genetics, anatomic abnormalities, diet, and other environmental factors).[8] Because crystalluria has not been observed in other MPS I colony cats, the concurrent renal failure and intratubular crystals suggest an association between these 2 processes. Tubular rupture associated with crystals in the interstitium support this theory. However, oxalate crystals can develop secondary to renal failure because of the inability of the diseased organ to process endogenous oxalates.[9] Therefore, the relationship between the crystals and the tubular necrosis is difficult to determine in the cat we present. Alternatively, tubular necrosis may have been secondary to the lysosomal storage disease. Although MPS I has not previously been associated with renal disease, the presence of numerous distended lysosomes in tubular epithelial cells with nuclear karyorrhexis suggests that the 2 could be related. Fabry disease, a lysosomal storage disease in which there is accumulation of glycolipid due to a deficiency in α-galactosidase, results in progressive renal failure, necessitating transplantation in humans.[2] If the degeneration and necrosis is secondary to the storage disease, the current case represents an atypical response of the tubular epithelial cells.

The increased number of interstitial macrophages was most likely a response to the tubular necrosis and rupture. Secretion of the macrophage chemotaxin, osteopontin, has been documented in damaged renal tubular epithelial cells.[11] In addition, osteopontin secretion has been associated with crystalluria, although whether it causes or prevents crystal formation is uncertain.[11] Unfortunately, immunohistochemistry using an antibody against rat osteopontin was unsuccessful in the current case because it did not crossreact with feline osteopontin. To our knowledge, antibodies against feline osteopontin are not commercially available.

Although either crystalluria or the accumulation of storage product in tubular epithelial cells may have been the primary insult, these 2 pathogeneses are not mutually exclusive. Furthermore, the interstitial expansion by distended macrophages likely played a role in the progression of the renal disease. A plausible scenario is one in which tubular necrosis secondary to crystalluria or storage substrate (or both) attracted GAG- and lipid-laden macrophages, which then caused tubular ischemia by increasing the distance between tubules and their blood supply and by compressing peritubular capillaries. Interstitial ex-

pansion that results in compression or rarefaction of peritubular capillaries is a well-recognized mechanism in the pathogenesis of tubulointerstitial injury.[7] Because other related cats have not had similar clinical courses or histologic lesions, the current case provides an unusual clinical presentation of a fairly well-characterized feline disease.

In conclusion, the case we present demonstrates for the first time the involvement of MPS I in the development of renal disease. After the initial renal damage, the presence of macrophages laden with storage product likely exacerbated tubular degeneration and necrosis, resulting in acute renal failure. Furthermore, this case report documents the diagnostic steps taken to investigate the cause of feline acute renal failure in a laboratory animal colony, allowing determination of the risk to other colony cats.

Acknowledgments

The work was supported by NIH grants DK25759 and RR02512.

References

1. **Bach G, Friedman R, Weissman B, Neufeld EF.** 1972. The defect in Hurler and Scheie syndromes: deficiency of α-L-iduronidase. Proc Natl Acad Sci USA **69:**2048–2051.
2. **Breunig F, Wanner C.** 2008. Update on Fabry disease: kidney involvement, renal progression, and enzyme replacement therapy. J Nephrol **21:**32–37.
3. **Clarke LA, Russell CS, Pownall S, Warrington CL, Borowski A, Dimmick JE, Toone J, Jirik FR.** 1997. Murine mucopolysaccharidosis type I: targets disruption of the murine α-L-iduronidase gene. Hum Mol Genet **6:**503–511.
4. **Haskins ME, Aguirre GD, Jezyk PF, Desnick RJ, Patterson DF.** 1983. The pathology of the feline model of mucopolysaccharidosis I. Am J Pathol **112:**27–36.
5. **Horton MA, Fowler P, Simpson A, Onions D.** 1988. Monoclonal antibodies to human antigens recognize feline myeloid cells. Vet Immunol Immunopathol **18:**213–217.
6. **Liang CT, Barnes J.** 1995. Renal expression of osteopontin and alkaline phosphatatse correlates with BUN levels in aged rats. Am J Physiol **269:**398–404.
7. **Nangaku M.** 2006. Chronic hypoxia and tubulointerstitial injury: a final common pathway to end-stage renal failure. J Am Soc Nephrol **17:**17–25.
8. **Osborne CA, Lulich JP, Kruger JM, Ulrich LK, Koehler LA .** 2008. Analysis of 451,891 canine uroliths, feline uroliths, and feline urethral plugs from 1981–2007: perspectives from the Minnesota Urolith Center. Vet Clin North Am Small Anim Pract **39:**183–197.
9. **Solez K, Racusen LC, Marcussen N, Slatnik I, Keown P, Burdick JF, Olsen S.** 1993. Morphology of ischemic acute renal failure, normal function, and cyclosporine-treated renal allograft recipients. Kidney Int **43:**1058–1067.
10. **Spellacy E, Schull RM, Constantopoulos G, Neufeld EF.** 1983. A canine model of human α-L-iduronidase deficiency. Proc Natl Acad Sci USA **80:**6091–6095.
11. **Xie Y, Sakatsume M, Nishi S, Narita I, Arakawa M, Gejyo F.** 2001. Expression, roles, receptors, and regulation of osteopontin in the kidney. Kidney Int **60:**1645–1657.